Aswan University Journal of Science and Technology Volume 4, issue 3

Structural Behavior of Concrete Beams Strengthened with Near-Surface-Mounted BFRP Reinforcement

Mohamed kamal eldin[1], Zakaria Hameed Awadallah[2], Mohamed Mahmoud Ahmed[3], Mohamed Zakaria Abdelhamed[1]
[1]Civil Engineering Department, Faculty of Engineering, Aswan University, Aswan, Egypt.
[2]Assistant Professor, Department of Civil Engineering, Al-Azhar University, Egypt.
[2]Civil Engineering Department, Faculty of Engineering, Assiut University, Assiut Egypt.

Abstract: This study explored the behavior of reinforced concrete (RC) beams when reinforced with Basalt Fiber Reinforced Polymers (BFRP) bars using the Near-Surface-Mounted (NSM) technique. BFRP is a recently developed material known for its cost-effectiveness, high strength, and exceptional corrosion resistance, making it an attractive option for reinforcing and repairing RC structures. The experiment involved four RC beams, with one serving as a reference and three strengthened with BFRP bars via NSM. These beams underwent a four-point bending test to evaluate their performance. The research focused on two critical parameters: the BFRP reinforcement ratio and the embedment length, analyzing their effects on load-carrying capacity, mid-span deflection, crack patterns, and final failure modes of the beams. The results shed light on the influence of these parameters on the behavior and strength of the beams, providing valuable insights for optimizing BFRP reinforcement strategies in enhancing the resilience and longevity of RC structures. The test results indicate an increase in the ultimate load of 22% to 33% compared with the control beam.

Keywords: Strengthening; RC Beams; Near Surface Mounted; Basalt Fiber Reinforced Polymers.

1. Introduction:

Concrete structures in Middle Eastern countries and various global regions face challenging environmental conditions, including extreme heat, humidity, and exposure to seawater, particularly evident in Egypt's coastal provinces. In comparison to traditional reinforcement materials, Fiber Reinforced Polymer (FRP) has emerged as a superior choice for reinforcing and repairing concrete structures. This preference arises from its advantageous characteristics, such as a low weight-to-

Corresponding author E-mail: eng.mohamedkelaraby@gmail.com

Received April 23, 2024, received in revised form, May 21, 2024, accepted May 30, 2024.
(ASWJST 2021/ printed ISSN: 2735-3087 and on-line ISSN: 2735-3095) https://journals.aswu.edu.eg/stjournal

volume ratio that facilitates easier application, a high strength-to-weight ratio, and corrosion resistance, ultimately enhancing the durability of reinforced concrete structures. Furthermore, FRP exhibits notable fatigue strength when subjected to repeated loading, making FRP bars suitable for use as internal reinforcement or as Near Surface Mounted (NSM) rebar [1].

Many studies have confirmed that FRP offers several advantages over steel as NSM reinforcement, including enhanced corrosion resistance, faster installation due to its lightweight nature, and reduced groove size [2-4].

The Near Surface Mounted (NSM) technique entails inserting FRP bars or strips into pre-cut grooves within the concrete cover within a tension zone, which is then filled with high-strength epoxy adhesive. This approach is straightforward and significantly improves the adhesion of the FRP reinforcement, optimizing the material's utilization. The depth of the concrete cover dictates the arrangement of the FRP reinforcement employed in NSM technology [5].

Rami H. Haddad et al. [6] investigated the flexural performance and failure modes of concrete beams strengthened with near-surface mounted (NSM) carbon fiber reinforced polymer (CFRP) strips. They conducted tests on 19 reinforced concrete beams (150 × 250 × 1400 mm) with a consistent longitudinal steel reinforcement ratio of 1%, and shear reinforcement was determined based on a constant shear/flexural theoretical ultimate load capacity ratio of approximately 1.5. The primary considered parameters were varying embedment lengths, numbers of strips, spacing, and positioning relative to the primary steel. The researchers observed that the residual ultimate load capacity and rotational ductility reached their peak and nadir at an embedment length of 450 mm, recording 154% and 85%, respectively. The introduction of staggered NSM CFRP strips in strengthened beams led to enhancements in residual flexural capacity and toughness by up to 30% and 51%, respectively. However, this improvement came at the expense of a slight 6% reduction in stiffness compared to the scenario without staggered strips.

Guohua Xing et al. [7] investigated the flexural behavior of RC beams strengthened with Near-Surface-Mounted Basalt Fiber Reinforced Polymer (BFRP) bars. The study involved testing one reference beam and six beams reinforced with NSM BFRP reinforcements under four-point loading conditions. The main studied variables included the NSM reinforcement ratio, tensile reinforcement ratio, and pre-cracking load. Seven RC beams were specifically crafted to examine the impact of BFRP reinforcement ratio, tensile steel reinforcement ratio, and pre-cracking load on the flexural performance of NSM BFRP-strengthened beams. The overall behavior of RC beams reinforced with NSM BFRP demonstrated that the maximum load of pre-cracked strengthened RC

specimens decreased by an average of 27.8% compared to directly strengthened specimens.

Previous studies have demonstrated the efficacy of BFRP as a robust strengthening material. The objective of the present research is to validate and further substantiate these findings while systematically addressing a broader spectrum of parameters. This approach aims to enhance the comprehensive understanding and potential applications of BFRP in diverse structural strengthening contexts.

2. Experimental program:

2.1 Material proportions and Mix proportion

Ordinary Portland Cement (Cemex) was used in all mixtures and tested it according to the Egyptian Code of Practice [8]. tap water, coarse aggregate with 20 mm maximum aggregate size, and Clean and round fine aggregate were used. A commercial superplasticizer (ADDICRETE BVF) was added to the mixture to achieve the target workability. A concrete mix was designed to give concrete compressive strength about 30 MPa after 28-days ago, and a slump of about 75 mm. The mixture's proportions of cement, coarse aggregate, fine aggregate, water, and superplasticizer were 400, 1300, 610, 180, and 3 kg/m3, respectively.

2.2 Test Specimens

The experimental methodology involved the examination of four reinforced concrete beams, including one control beam and five beams reinforced for enhanced strength. These beams were subjected to simple support conditions and exposed to two concentrated static loads until reaching failure. The beams featured a rectangular cross-sectional profile measuring 200 by 300 millimeters, spanning a total length of 2100 millimeters. Each beam was reinforced with two compression bars with a diameter of 10 millimeters and two tension bars with a diameter of 12 millimeters. Additionally, shear reinforcement was provided using 8 millimeter plain bars spaced at intervals of 125 millimeters. The concrete utilized in all beams demonstrated a comparable compressive strength of approximately 30 megapascals, as depicted in Figure 1: 4. Concrete compressive strength was assessed by conducting tests on three 150 millimeter cubes extracted during the casting process. A concise overview of the average compressive strength (f_{cu}) and the complete testing protocol is delineated in Table 1, Before building all the cages and placing them in the mold, the foam pieces (25mm wide x 25mm deep) were fastened to the bottom of the mold to form the grooves for the NSM reinforcement beams as shown in Figure 5.

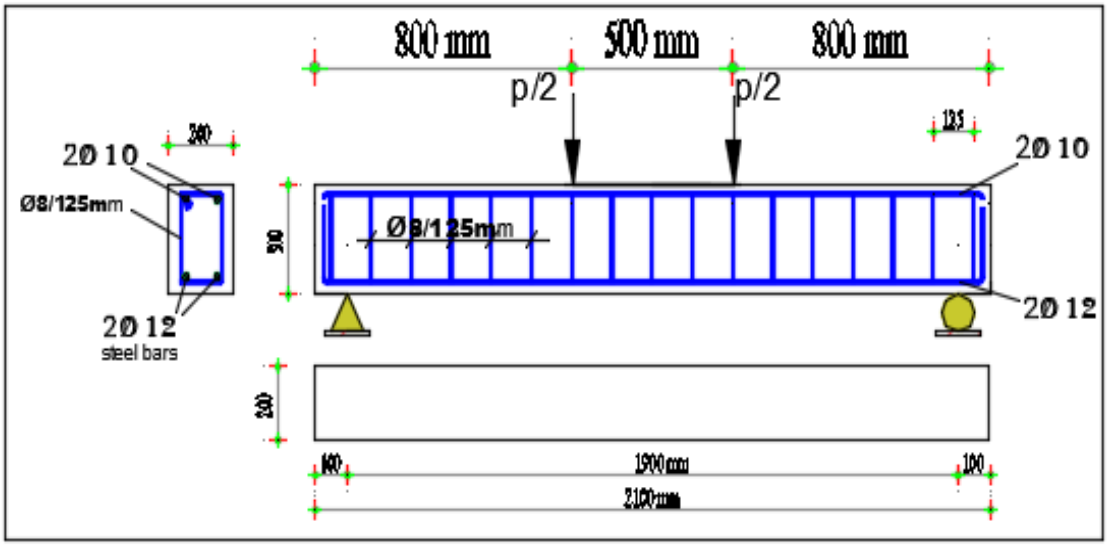

Fig. 1 Details of the control beam as illustrated by bottom and cross-sectional views of the concrete beams.

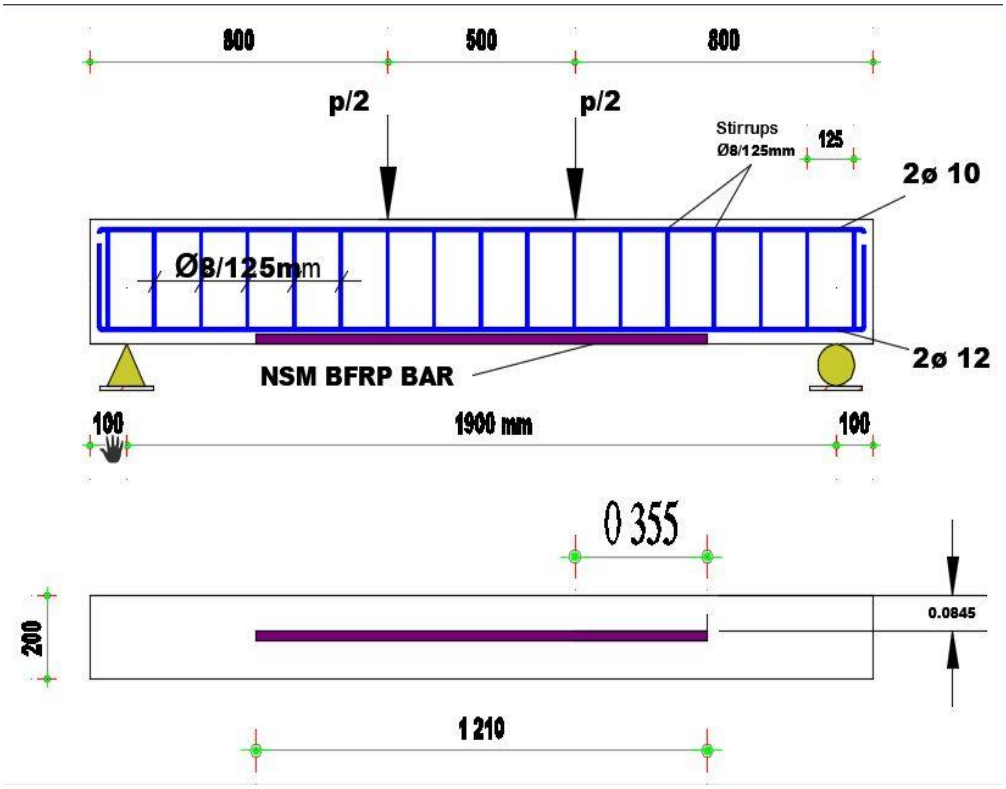

Fig. 2 Details of beam NSM1 as illustrated by bottom.

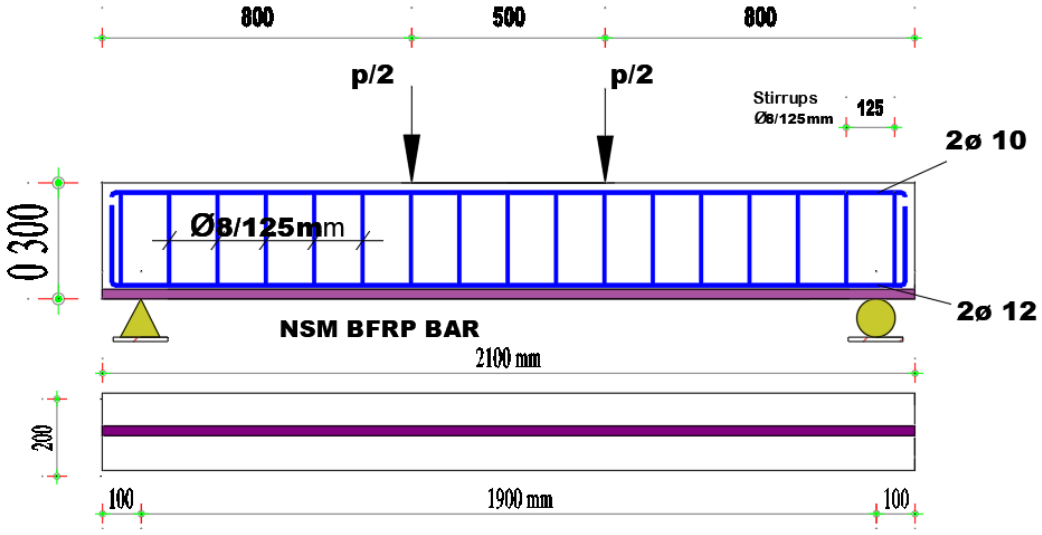

Fig. 3 Details of beam NSM3 as illustrated by bottom.

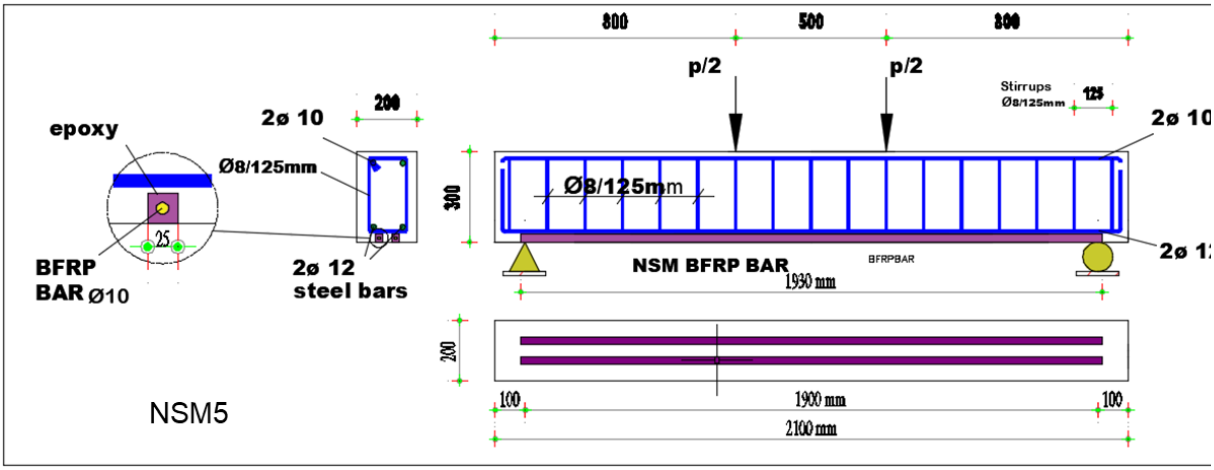

Fig. 4 Details of beam NSM5 as illustrated by bottom and cross-sectional views of the concrete beams.

Table 1 Designation of test specimens and parameters

NO.	Name	f_{cu}	CR (mm)	TR (mm)	FR (mm)	FL (m)	EL (m)
1	CB	38.1	2Ø10	2Ø12	-----	-----	-----
2	NSM1	33.5	2Ø10	2Ø12	1Ø10	1.21	(0.355)
3	NSM3	33.4	2Ø10	2Ø12	1Ø10	2.10	(0.800)
4	NSM5	33.1	2Ø10	2Ø12	2Ø10	1.93	(0.715)

f_{cu} is the compressive strength of the concrete, CR is the Compression reinforcement, TR is the Tension reinforcement, FR is the FRP reinforcement, FL is the FRP Length, and EL is the Embedment length beyond the maximum moment zone.

2.3 BFRP Composites

The results of the tested BFRP bars as three samples of diameter have been formed on each of them, according to the Egyptian standard. The results of the tests are as follows shown in Table 2 and their prescribed adhesives from Prokem were used to strengthen the different samples. Adhesive properties, as provided by the manufacturer (Prokem) of the CFT epoxy adhesive, are shown in Table 3.

Table 2 Properties of BFRP bars

Original diameter (mm)	Original length (cm)	Final length(cm)	Yield load (ton)	Maximum load (ton)	Breaking load (ton)	Yield stress (MPa)
10	8.5	---	----	4.8	----	----
10	8.5	10.5	6	12	9	1528.66
10	9.5	11	5	9.5	9	1210.19

Table 3 Properties CFT adhesive epoxy used for bonding BFRP strips

Mixed density at 23 °C	1.55 ±0.05 g/cm^3
Modulus of elasticity	2500 N/mm^2
Bond to concrete	3 N/mm^2
Tensile strength	30-35 N/mm^2
Flexural strength	40-45 N/mm^2
Adhesion stress	60 N/mm^2

Fig. 5. The foam pieces (25mm wide x 25mm deep)

For all strengthened beams, the grooves were cleaned from dust and loose materials before inserting the FRP bars. The two components of the epoxy resin were pre-mixed and the mixture was added to the beam's grooves before/after installation of the FRP bars. Figure 6 shows some of the NSM beams after the installation of the bars.

Fig. 6 Beams after the installation of the NSM bars.

2.4 Test set-up and instrumentation

All the strengthened specimens were tested in four-point bending using a hydraulic actuator with a capacity of 1000 kN. The loading was applied under a hydraulic actuator at a speed of (1

mm/min) using an actuator. The measurement of all test data was recorded using a static data logger and a computer at intervals of 1 second. A load cell was installed between the hydraulic actuator and the steel plate to accurately monitor and record the applied load during testing. The loading points and supports were selected to provide an effective span of 1900 mm and a shear span of 500 mm. The vertical mid-span deflection of the specimens during the test was recorded by linear voltage displacement transducers (LVDT). Three strain gauges were instrumented to monitor strains in the steel bars and BFRP bars at the mid-span section of the beams. One of the strain gauges was attached to one tensile steel bar (before casting) and the other two strain gauges were attached to two selected BFRP bars. The strains in the concrete at the mid-span along the cross-section were also measured by one concrete strain gauge. All measurement devices were connected to a high-speed data acquisition system to acquire the data and monitor the response of the tested specimens (static data logger). In addition, crack widths were recorded manually at each loading step and the corresponding applied loads were recorded near the marked cracks on the surface of each beam specimen. Figure 7 shows the test setup and instrumentation.

Fig. 7 Test set-up.

3. Results and Discussion:

The analysis of specimen behavior encompasses various aspects, including the failure history leading up to the final failure, the mode of failure, capacity considerations such as strength and deformation (deflection), the strain distribution within main member components, and the patterns of crack formation. It is crucial to discuss key observations made during the quasi-static tests of the beams to enhance understanding of the behavior of RC beams reinforced with BFRP bars using the NSM technique. Table 4 presents important findings regarding the investigated specimens under quasi-static loads, juxtaposed with those of the control beam.

Table 4 Test results of examined specimens.

Beam Specimen	Specimen Designation	P_{cr} (ton)	P_u (ton)	Δ_{cr} (mm)	Δ_{max} (mm)
CB	CB	3.125	12.875(100%)	0.934	28.66
NSM1	NSM1-1/10/35.5	3.00	14.000(109%)	0.891	15.72
NSM3	NSM3-1/10/80	3.75	15.750(122%)	1.980	28.91
NSM5	NSM5-2/10/71.5	3	17.125(133%)	0.780	18.858

P_{cr} corresponds to the cracking load, P_u is the ultimate load, Δ_{cr} is the deflection corresponding to the cracking load, and Δ_{max} is the maximum deflection corresponding to the ultimate load for Specimens.

3.1 Ultimate Load

Concerning the control reinforced beam, Fig. 8 demonstrates the efficacy of the NSM technique utilizing BFRP bars in augmenting the strength capacity of retrofitted beams. Parameters such as the embedment length of the bars, their extension beyond the point where the moment begins to decrease, the reinforcement ratio, and the arrangement of the BFRP bars are pivotal in determining this enhancement. Notably, the strength capacity ratio exhibited an approximate 9% increase compared to that of the control beam when employing a minimum BFRP reinforcement ratio and shorter embedded length (NSM1-1/10/35.5). Furthermore, achieving full anchorage of the bars can further amplify the strength capacity, as evidenced in specimens NSM1-1/10/35.5 and NSM3-1/10/80.

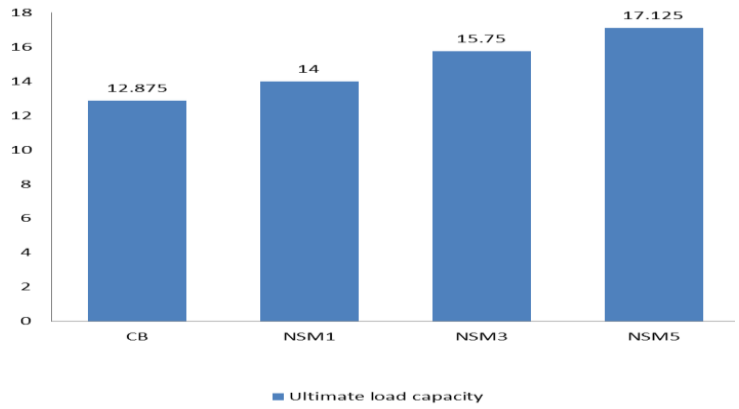

Fig. 8 Ultimate load of tested beams.

3.2 Deflection

3.2.1 Effect of the BFRP Reinforcement Ratio.

Figure 9 illustrates the deflection results for beams CB, NSM3, and NSM5, considering different BFRP reinforcement ratios, depicted through load-deflection curves. Initially, all beams exhibit linear shear load-deflection behavior until reaching the cracking load, at which point cracking occurs in the zone of maximum moment, resulting in a reduction in stiffness. Notably, it was observed that beam NSM5 consistently demonstrated lower deflection values compared to beams CB and NSM3.

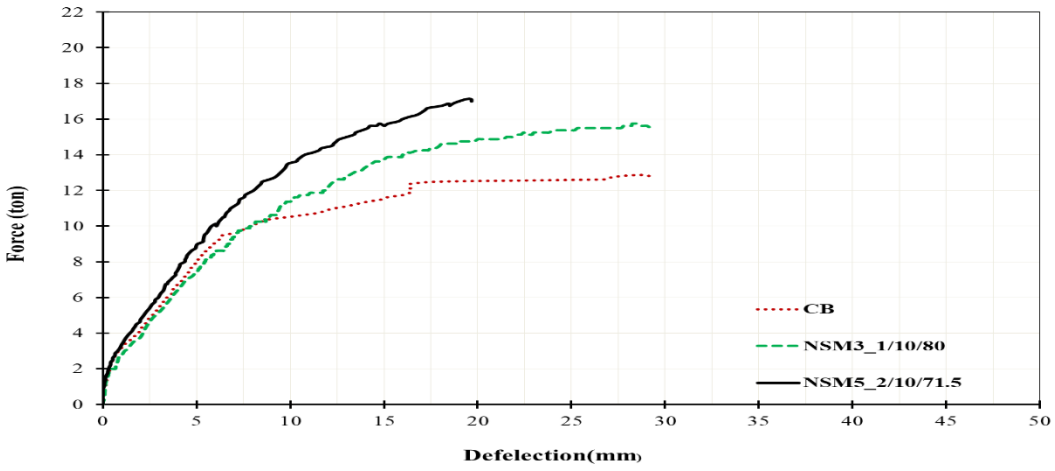

Fig. 9 Load–deflection curves for tested beams (CB, NSM3, and NSM5).

3.2.2 Effect of Embedment Length Ordinary Model

Figure 10 shows the load-deflection curves for various beams, reinforced with a single NSM BFRP bar with embedment lengths of 355 mm for NSM1 and 800 mm for NSM3, respectively, in comparison to control (CB) beams. Initially, the curves exhibit linear behavior during the initial loading stages, transitioning to nonlinear behavior thereafter. However, due to the short embedment length of the BFRP bar (35.5cm), deponding of the bar was observed at a maximum load of about 14 tons and a mid-span deflection of about 15.72mm, the flexural failure was associated with a maximum deflection of almost 28.91mm. Moreover, the first crack initiated at a load being 3.75 ton and was consistent with a recorded deflection of almost 1.98mm as shown in Figure 10. Beams reinforced with NSM BFRP with embedment lengths of 355 mm and 800 mm achieve load capacities 109% and 122% greater than those of control beams, respectively, indicating the advantage of extending NSM BFRP bars beyond the high moment zone. The characteristics of these beams are summarized in Table 4.

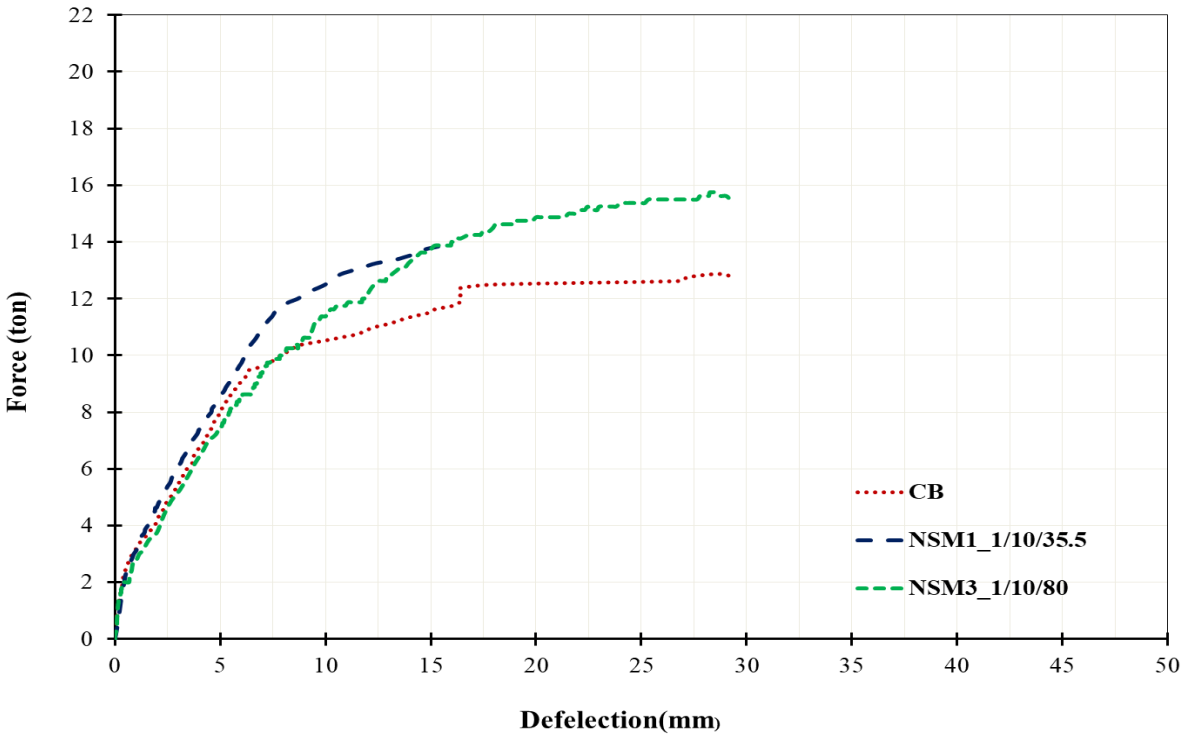

Fig. 10 Load–deflection relationships for beams (NSM1 and NSM3).

3.3 Crack patterns and Mode of Failure

3.3.1 Effect of the BFRP Reinforcement Ratio.

The effect of the BFRP reinforcement ratio on crack patterns in beams (CB, NSM3, and NSM5)

is illustrated in Figure 11. As the reinforcement ratio of BFRP bars increases, both the number and height of cracks at equivalent loading levels decrease. Moreover, higher reinforcement ratios result in smaller crack widths under identical loading conditions. This increase in reinforcement ratio (ρ_f %) also influences the aggregate interlock capacity. Beams with lower reinforcement ratios, such as NSM3, exhibit wide and lengthy cracks, contrasting with the shorter and narrower cracks observed in beams with higher reinforcement ratios. Since the aggregate interlock mechanism relies on crack width, an augmentation in aggregate interlock force can be anticipated with an increase in reinforcement ratio (ρ_f %). The mode of failure in beams NSM3 and NSM5 was identified as shear failure, whereas in beam CB, it was characterized by flexural failure with concrete crushing.

a) Crack pattern and mode of failure for beam (CB).

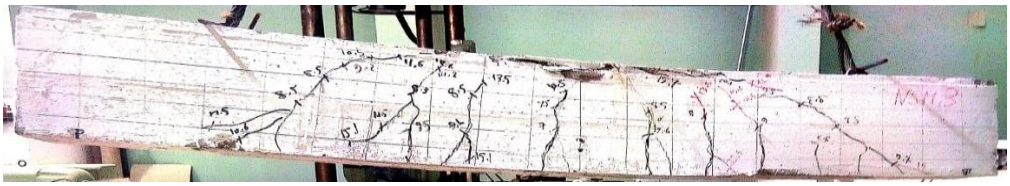

b) Crack pattern and mode of failure for beam (NSM3).

c) Crack pattern and mode of failure for beam (NSM5).

Photo 1. Crack pattern and mode of failure for beams with different reinforcement ratios of BFRP bars, (ρ_f %).

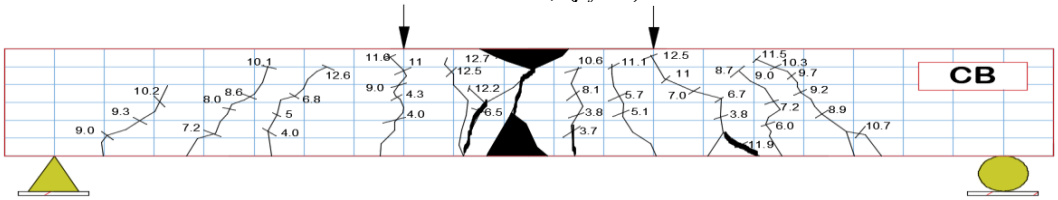

a) Crack pattern and mode of failure for beam (CB).

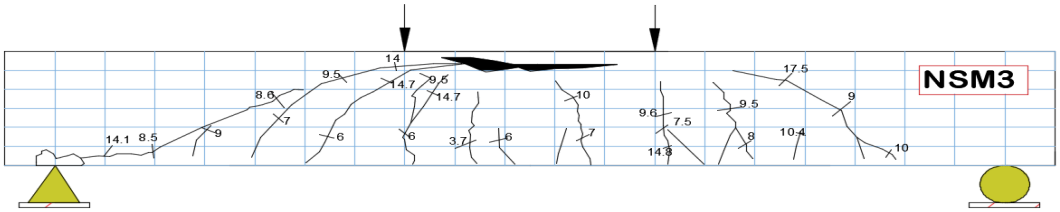

b) Crack pattern and mode of failure for beam (NSM3).

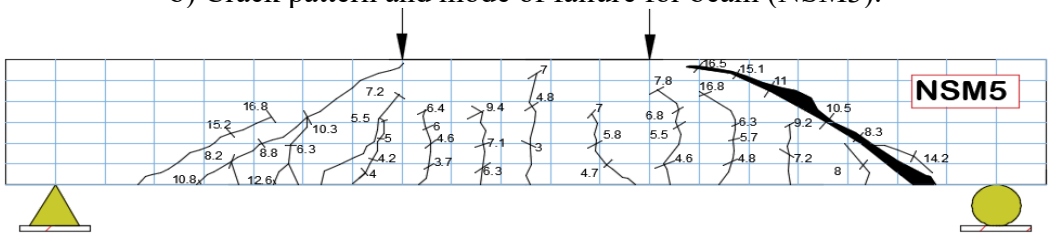

c) Crack pattern and mode of failure for beam (NSM5).

Fig. 11 Crack pattern and mode of failure for beams with different reinforcement ratios of BFRP bars, (ρ_f %).

3.3.2 Effect of Embedment Length Ordinary Model.

The failure modes of beams, reinforced with one NSM BFRP bar for NSM1 and NSM3 at embedment lengths of 355 mm and 800 mm, respectively, are depicted in Figure 12 As the load is applied, flexural cracks initiate at the middle zone, occurring at loads of 30 kN and 37.5 kN, respectively, before spreading across the entire span. After further loading, end-cover separation begins with the development of vertical cracks across the concrete cover at the termination points of the NSM BFRP bars, observed at loads of 115 kN and 120 kN, respectively. In the case of beam NSM1, this is followed by the progression of a major horizontal crack at the level of the tension reinforcement towards the high-tension zone, while for beam NSM3, failure occurs in a combination of flexural and concrete crushing.

a) Crack pattern and mode of failure for beam (NSM1).

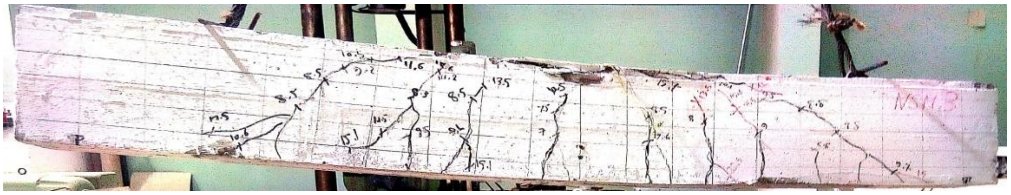

b) Crack pattern and mode of failure for beam (NSM3).

Photo 2 Crack pattern and mode of failure for beams with different Embedment length when strengthened with one NSM BFRP bar.

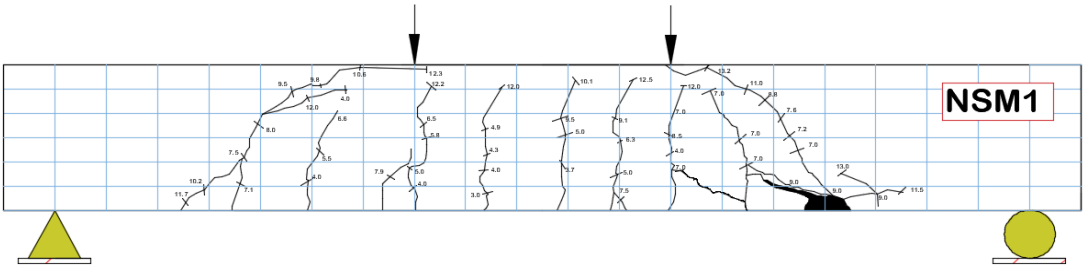

a) Crack pattern and mode of failure for beam (NSM1).

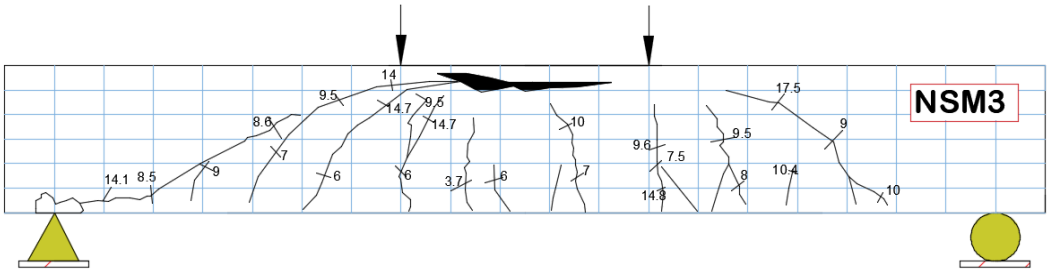

b) Crack pattern and mode of failure for beam (NSM3).

Fig. 12 Crack pattern and mode of failure for beams with different Embedment length when strengthened with one NSM BFRP bar.

4. conclusion

To investigate the flexural behavior of RC beams strengthened with BFRP bars, four full-scale reinforced concrete beams measuring 200×300×2100 mm (width × depth × length) were constructed and reinforced with various types of BFRP bars. The experimental parameters encompassed the strengthening technique (NSM) and the type of FRP used (Basalt). Based on the test results of this study, the following conclusions can be drawn:

All reinforced beams exhibited an increase in ultimate capacity compared to the reference beam, with enhancements ranging between 109% and 133%.

- Beams reinforced with NSM-BFRP displayed excellent ductile behavior, showcasing high deflection values at ultimate load that were comparable to or even greater than those recorded in the reference beam. This characteristic provides ample warning before failure and can be deemed a significant advantage of utilizing BFRP bars in the NSM strengthening technique.

- Debonding has emerged as a significant challenge in the NSM-FRP method. This study observed that most reinforced beams experienced sudden debonding failures, while NSM-BFRP beams demonstrated favorable ductile characteristics. Further investigation

is necessary to develop effective strategies for mitigating debonding problems in the NSM-FRP technique.

- Additionally, it is recommended to conduct more comprehensive studies on the utilization of BFRP bars as NSM reinforcement, as it substantially enhances capacity and demonstrates favorable ductile behavior.

REFERENCES

[1] M. A. Badawi, "Monotonic and fatigue flexural behaviour of RC beams strengthened with prestressed NSM CFRP rods," 2007.

[2] L. De Lorenzis, A. Nanni, and A. La Tegola, "Strengthening of reinforced concrete structures with near surface mounted FRP rods," in *International meeting on composite materials, PLAST*, 2000, pp. 9-11: Citeseer.

[3] S. M. Soliman, E. El-Salakawy, and B. Benmokrane, "Flexural behaviour of concrete beams strengthened with near surface mounted fibre reinforced polymer bars," *Canadian Journal of Civil Engineering,* vol. 37, no. 10, pp. 1371-1382, 2010.

[4] R. Parretti and A. Nanni, "Strengthening of RC members using near-surface mounted FRP composites: Design overview," *Advances in structural engineering,* vol. 7, no. 6, pp. 469-483, 2004.

[5] S. El-Gamal, A. Al-Nuaimi, A. Al-Saidy, and A. Al-Lawati, "Flexural strengthening of RC beams using near surface mounted fibre reinforced polymers," in *5th Brunei International Conference on Engineering and Technology (BICET 2014)*, 2014, pp. 1-7: IET.

[6] R. H. Haddad and O. A. Almomani, "Flexural performance and failure modes of NSM CFRP-strengthened concrete beams: a parametric study," *International Journal of Civil Engineering,* vol. 17, no. 7, pp. 935-948, 2019.

[7] G. Xing, Z. Chang, and Z. Bai, "Flexural behaviour of RC beams strengthened with near-surface-mounted BFRP bars," *Magazine of Concrete Research,* vol. 70, no. 11, pp. 570-582, 2018.

[8] E. C. Committee, "ECP-203," *Egyptian Code for Design and Construction of concrete Structures, HBRC, Giza, Egypt,* 2018.